

# Experimental Studies of Ozone Depletion by Chlorofluorocarbons (CFC's), Bromofluorocarbons (BFC's), Hydrochlorofluorocarbons (HCFC's), and CH<sub>3</sub>Br Using a 6-m<sup>3</sup> Photochemical Chamber

Nobuaki Washida,\* Takashi Imamura, and Hiroshi Bandow<sup>#</sup>

Division of Atmospheric Environment, The National Institute for Environmental Studies,  
16-2 Onogawa, Tsukuba, Ibaraki 305

(Received June 15, 1995)

Ozone destruction by CFC's (CFCl<sub>3</sub> and CF<sub>2</sub>Cl<sub>2</sub>), BFC's (CF<sub>3</sub>Br and C<sub>2</sub>F<sub>4</sub>Br<sub>2</sub>), HCFC's (CH<sub>3</sub>CCl<sub>2</sub>F, CF<sub>3</sub>CHCl<sub>2</sub>, and CF<sub>3</sub>CHFCl), and CH<sub>3</sub>Br was demonstrated using a 6-m<sup>3</sup> evacuable photochemical chamber equipped with UV-enhanced Xe arc lamps. The decay of ozone by a catalytic cycle involving Cl or Br atoms released from the photolysis of halocarbons by UV light was evident, although the chain length was far less than that in the real stratosphere: It was about 8 for CFCl<sub>3</sub> and 40 for CF<sub>3</sub>Br. The rates of ozone decomposition were faster in the BFC's than in the CFC's. According to a box-model simulation, in the CFCl<sub>3</sub> system 90% of the catalytic cycle proceeds from reactions of Cl + O<sub>3</sub> → ClO + O<sub>2</sub> and ClO + O → Cl + O<sub>2</sub>. On the other hand, in the CF<sub>3</sub>Br system 90% of the catalytic cycle is governed by the following reactions: Br + O<sub>3</sub> → BrO + O<sub>2</sub> and BrO + BrO → 2Br + O<sub>2</sub>. The HCFC's and CH<sub>3</sub>Br can destroy the ozone with sufficient potential as CFC's and BFC's when they enter the stratosphere.

Since the first prediction by Molina and Rowland,<sup>1)</sup> it is well known that stratospheric ozone is destroyed by a catalytic cycle involving Cl or Br atoms released from the photolysis of chlorofluorocarbons (CFC's) or bromofluorocarbons (BFC's) by sunlight. Studies concerning the destruction of stratospheric ozone have been carried out involving the determination of the rate constants and reaction mechanisms of the photodecomposition of the CFC's and BFC's as well as the elementary processes of the catalytic reactions,<sup>2)</sup> also, computer model calculations based on a variety of scenarios<sup>3)</sup> were made.

However, ozone depletion due to such catalytic reactions has never been demonstrated. In the present study, experiments concerning ozone depletion were carried out in a 6-m<sup>3</sup> evacuable photochemical chamber, in which selected CFC's and BFC's were added to about 5 ppm O<sub>3</sub> diluted in about 50 Torr (1 Torr = 133.322 Pa) air and irradiated by UV light. The decay of ozone, which was observed in all cases, is reported. The same experiments were also carried out for the HCFC's (hydrochlorofluorocarbons) and methyl bromide. The decay rates of ozone by each compound are summarized and evaluated.

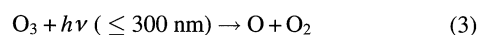
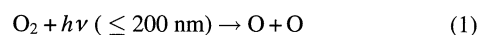
## Experimental

All of the experiments were carried out in an evacuable photochemical chamber (6 m<sup>3</sup>), whose inner surface was coated with tetrafluoroethylene-perfluoroalkyl vinyl ether copolymer (PFA). Details concerning this chamber have already been reported.<sup>4)</sup> The solar simulator and the end windows used to introduce UV light

<sup>#</sup>Present address: College of Engineering, University of Osaka Prefecture, 1-1 Gakuencho, Sakai, Osaka 593.

were modified in order to utilize shorter wavelength light for the effective photolysis of the CFC's. UV-enhanced Xe arc lamps (1000 W × 19 units) and synthetic quartz (Suprasil) windows were installed.<sup>5,6)</sup> The spectral distribution of the output of the UV-enhanced Xe arc lamps is shown in Fig. 1. The spectra were measured by the following procedures: 1) The chamber was evacuated to a vacuum. 2) The space from the Xe-arc lamps to the entrance windows of the chamber (about 3 m distance in order to collimate each light beam) was filled by flowing 1 atm air. 3) The spectra were measured at both sides of the chamber (in front of the entrance windows and behind the exit windows) by a Nikon (P-250) monochromator. 4) Both spectra were normalized and calibrated to radiometric standards. Since spectra shorter than 200 nm could not be calibrated, it is not shown in Fig. 1.

The ozone introduced into the photochemical chamber was prepared by two methods. One was the UV irradiation of air. The photostationary state concentration of ozone can be obtained by the photodecomposition of oxygen and ozone:



The photostationary state concentration of ozone was about 5 ppm (1 ppm = 10<sup>-4</sup>%) for 50 Torr (1 Torr = 133.322 Pa) of air when Xe arc lamps were used under normal operation. The other method was to supply ozone from a commercial ozonizer. Since several hours are necessary to obtain a photostationary state concentration of ozone by the UV irradiation of air, the latter method was mostly used in this study. Before conducting experiments the chamber was exposed by a high concentration of ozone in order to minimize the heterogeneous decay of ozone on the PFA wall. After this treatment,

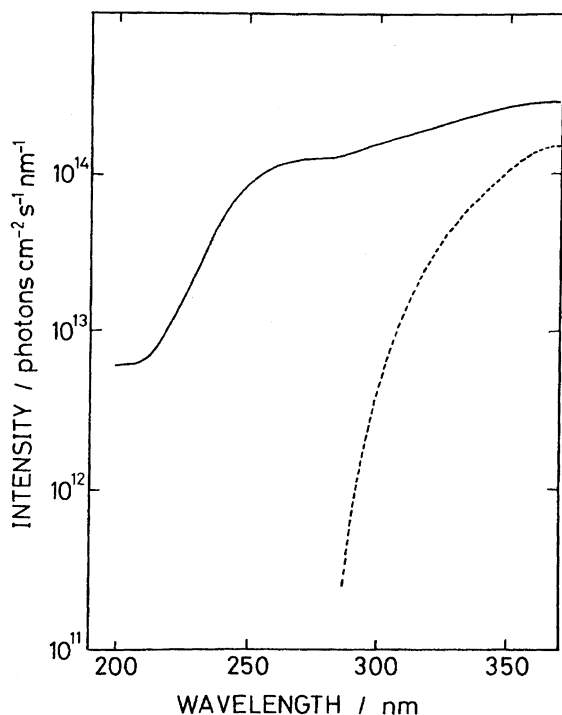


Fig. 1. The spectral distribution of the output of the UV-enhanced Xe arc lamps (bandwidth 5nm) and the estimated actinic irradiance. The dotted line shows the solar simulator used before for the tropospheric study.

the decay rate of ozone without irradiation was kept to be less than  $2 \times 10^{-3} \text{ min}^{-1}$ . The concentration of ozone was monitored through UV absorption coupled with the phase-shift method by the 253.7 nm mercury line.

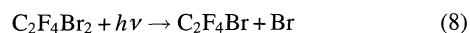
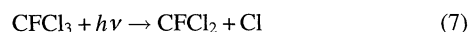
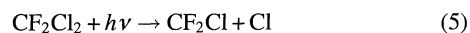
The concentrations of the reactants of the CFC's, BFC's, HCFC's, and  $\text{CH}_3\text{Br}$  were measured by means of long-path Fourier transform infrared spectroscopy (FT-IR) (Fuji-Electronic Co, FIRIS-100Z; path length, 221.5 m; resolution,  $1 \text{ cm}^{-1}$ ) utilizing multireflection mirrors installed in the chamber. The typical reagent concentrations were as follows:  $[\text{O}_3] = 5\text{--}8 \text{ ppm}$ ,  $[\text{halocarbon}] = 0.8\text{--}50 \text{ ppm}$ , and purified air of 50 Torr (corresponding to the atmospheric pressure at ca. 20 km altitude in the stratosphere). The gases in the chamber were stirred by two mechanical fans. All of the gases, ( $\text{CFCl}_3$ ,  $\text{CF}_2\text{Cl}_2$ ,  $\text{CF}_3\text{Br}$ ,  $\text{C}_2\text{F}_4\text{Br}_2$ ,  $\text{CH}_3\text{CCl}_2\text{F}$ ,  $\text{CF}_3\text{CHCl}_2$ ,  $\text{CF}_3\text{CHFCl}$ , and  $\text{CH}_3\text{Br}$ ) were used as delivered. The air was supplied by an air purifier (Standard Technology Inc., SGPU-21) in which hydrocarbons and NO in source air were converted to  $\text{CO}_2$ ,  $\text{H}_2\text{O}$ , and  $\text{NO}_2$  by a  $\text{Pt}/\text{Al}_2\text{O}_3$  catalyst at  $450^\circ\text{C}$ ; also,  $\text{CO}_2$ ,  $\text{H}_2\text{O}$ , and  $\text{NO}_2$  were removed by a molecular-sieve adsorbent. All of the experiments were carried out at  $30 \pm 1^\circ\text{C}$ .

## Results and Discussion

**1) Measurements of the Photodissociation Rates of CFC's, BFC's, HCFC's, and  $\text{CH}_3\text{Br}$ .** It is well known<sup>7)</sup> that an optical window exists in the stratosphere at wavelengths of 190–210 nm (between two principal absorption regimes of oxygen and ozone, respectively), where solar radiation reaches deeper into the atmosphere, and that radiation in the window region is responsible for the photodissociation of minor constituents, such as halocarbons, in the atmosphere. As shown in Fig. 1, the output of the Xe arc lamps

used in this study covered the window region, although the spectral distribution of the Xe arc lamps is not quite similar to real solar radiation in this window region.

First, measurements of the photodissociation rates of the halocarbons used in this study by irradiating Xe arc lamps were determined under the condition of 100 Torr  $\text{N}_2$ . The results for the CFC's and BFC's are shown in Fig. 2. The initial concentrations of  $\text{CF}_2\text{Cl}_2$ ,  $\text{CF}_3\text{Br}$ ,  $\text{CFCl}_3$ , and  $\text{C}_2\text{F}_4\text{Br}_2$  were 3.8, 19.2, 19.4 and 3.0 ppm, respectively. The decreases in the concentrations were measured by IR absorption. Figure 2 gives the values of the relative IR transmittance ( $I_t/I_0$ ), which are plotted against irradiation time (the scale of the ordinate is logarithmic). Here,  $I_0$  stands for the absorption before irradiation and  $I_t$  represents the absorption at the irradiation time ( $t$ ). From the slopes shown in Fig. 2, the photodissociation rates ( $J_x$ ) of  $\text{CF}_2\text{Cl}_2$ ,  $\text{CF}_3\text{Br}$ ,  $\text{CFCl}_3$ , and  $\text{C}_2\text{F}_4\text{Br}_2$  were obtained to be  $(1.2 \pm 0.1) \times 10^{-4}$ ,  $(4.4 \pm 0.1) \times 10^{-4}$ ,  $(7.3 \pm 0.4) \times 10^{-4}$ , and  $(5.0 \pm 0.1) \times 10^{-3} \text{ min}^{-1}$ , respectively. The photodissociation processes of the above compounds are thought to be as follows:



In all cases, halogen atoms released could not react with the parent halocarbons, and might have been lost on the walls of the chamber. Therefore, the values of  $J_x$  should be the real photodissociation rates of the above-mentioned compounds by the Xe arc lamps used in this study.

In the case of the HCFC's, Cl atoms formed by the photodecomposition reacted with the HCFC's. For example, in the case of  $\text{CH}_3\text{CFCl}_2$  (HCFC-141b), a formed Cl atom can abstract a hydrogen of  $\text{CH}_3\text{CFCl}_2$ :

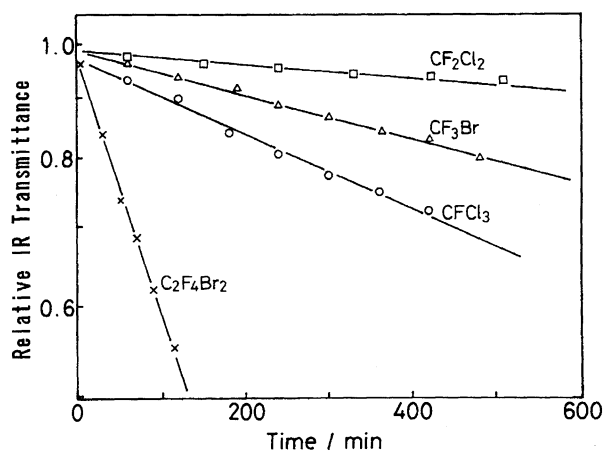
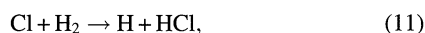


Fig. 2. Relative IR transmittance ( $I_t/I_0$ ) are plotted against irradiation time ( $t$ ) (scale of ordinate is logarithmic). Symbols;  $\text{CF}_2\text{Cl}_2$  ( $\square$ ),  $\text{CF}_3\text{Br}$  ( $\triangle$ ),  $\text{CFCl}_3$  ( $\circ$ ), and  $\text{C}_2\text{F}_4\text{Br}_2$  ( $\times$ ).

The rate constants for the reactions of the Cl atoms with the HCFC's have been reported<sup>2,8-10</sup> to be  $2.2 \times 10^{-15}$ ,  $1.2 \times 10^{-14}$ , and  $2.7 \times 10^{-15}$  cm<sup>3</sup> molecule<sup>-1</sup> s<sup>-1</sup> for CH<sub>3</sub>CFCl<sub>2</sub> (HCFC-141b), CF<sub>3</sub>CHCl<sub>2</sub> (HCFC-123), and CF<sub>3</sub>CHFCl (HCFC-124), respectively, at 298 K. Therefore, the decay of CH<sub>3</sub>CFCl<sub>2</sub> due to irradiation was not a single exponential, as was the case of CFC's and BFC's in Fig. 2.

In order to exclude secondary consumption of the HCFC's by Cl atoms, after adding about 1 Torr of hydrogen to the system, the photodecomposition rate was measured in a 50 Torr air system instead of nitrogen. In this system Cl atoms formed in reaction (9) reacted predominately with H<sub>2</sub>,



because the rate constant for reaction (11) is reported<sup>11</sup> to be  $1.6 \times 10^{-14}$  cm<sup>3</sup> molecule<sup>-1</sup> s<sup>-1</sup>, and the concentration of H<sub>2</sub> is 10<sup>3</sup>-times higher than that of the HCFC's. The hydrogen atoms produced according to reaction (11) reacted with O<sub>2</sub> in air, and formed HO<sub>2</sub> radicals,



The rates for the reactions of HO<sub>2</sub> radicals with the saturated HCFC's are expected to be very slow, although they are not known.

The photodecomposition rates of CH<sub>3</sub>CFCl<sub>2</sub>, CF<sub>3</sub>CHCl<sub>2</sub>, CF<sub>3</sub>CHFCl, and CH<sub>3</sub>Br were measured in the H<sub>2</sub>/air system; the results are shown in Fig. 3 along with that for CFCl<sub>3</sub> as a reference. From the slopes of the plots, the photodissociation rates ( $J_x$ ) of CH<sub>3</sub>CFCl<sub>2</sub>, CF<sub>3</sub>CHCl<sub>2</sub>, CF<sub>3</sub>CHFCl, CH<sub>3</sub>Br, and CFCl<sub>3</sub> (for reference) are  $(1.2 \pm 0.1) \times 10^{-3}$ ,  $(1.1 \pm 0.1) \times 10^{-3}$ ,  $(1.9 \pm 0.5) \times 10^{-4}$ ,  $(6.9 \pm 0.4) \times 10^{-3}$ , and  $(2.3 \pm 0.2) \times 10^{-3}$  min<sup>-1</sup>, respectively. The photodissociation processes of these compounds might be as follows (in the case of CH<sub>3</sub>CFCl<sub>2</sub>, reaction (9)):

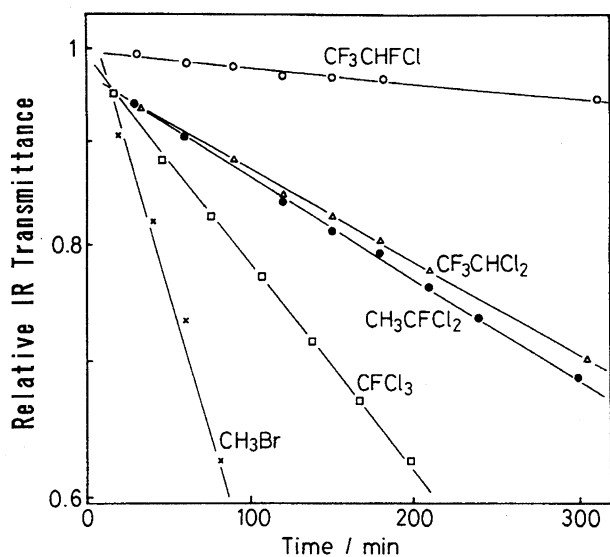
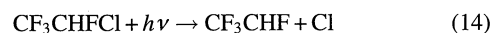


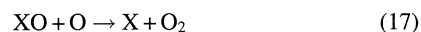
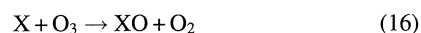
Fig. 3. Relative IR transmittance ( $I_t/I_0$ ) vs. irradiation time ( $t$ ). Symbols; CF<sub>3</sub>CHFCl (○), CF<sub>3</sub>CHCl<sub>2</sub> (△), CH<sub>3</sub>CFCl<sub>2</sub> (●), CFCl<sub>3</sub> (□), CH<sub>3</sub>Br (×). Scale of ordinate is logarithmic.



All of the results are summarized in Table 1.

## 2) Measurements of the Decay Rates of Ozone by the CFC's, BFC's, HCFC's, and CH<sub>3</sub>Br.

When a halo-carbon was added to the photostationary state concentration (PSSC) of ozone (described in Experimental section) under irradiation, a depletion of ozone, probably caused by the Cl or Br atom catalyzed chain reactions (16) and (17), was observed.



where, X is Cl or Br atoms.

The results obtained after adding CFCl<sub>3</sub> and CF<sub>3</sub>Br to the PSSC of O<sub>3</sub> are shown in Figs. 4 and 5. After a short induction period, ozone was destroyed rapidly in both cases.

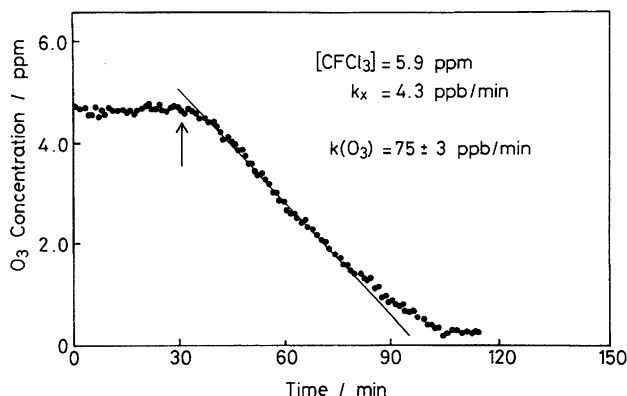


Fig. 4. Decay of the photostationary state concentration of ozone by the addition of 5.9 ppm of CFCl<sub>3</sub>. CFCl<sub>3</sub> was added at the time shown by an arrow. Slope gives the decay rate ( $k(\text{O}_3) = 75 \pm 3$  ppb min<sup>-1</sup>).

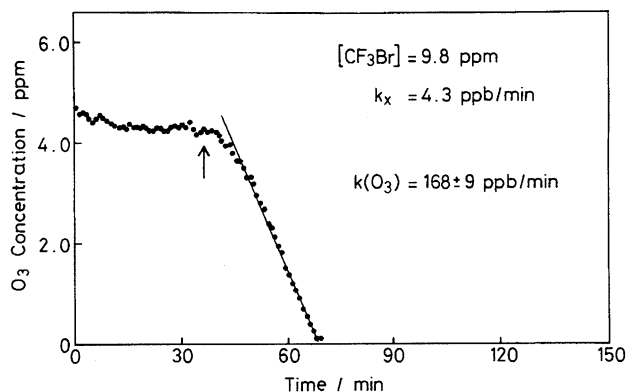


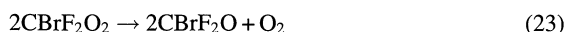
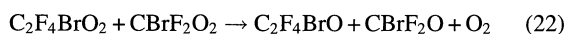
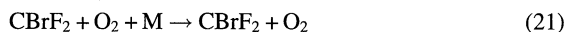
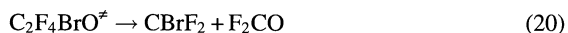
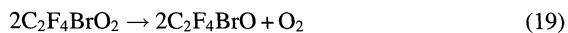
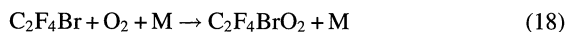
Fig. 5. Decay of the photostationary state concentration of ozone by the addition of 9.8 ppm of CF<sub>3</sub>Br. Formation rate of Br,  $k_x$  was adjusted to be as same as the case of CFCl<sub>3</sub> (Fig. 4). CF<sub>3</sub>Br was introduced at the time shown by an arrow. Slope gives the decay rate ( $k(\text{O}_3) = 168 \pm 9$  ppb min<sup>-1</sup>).

Table 1. Results of the Photodecomposition Rate ( $J_x$ ) and Ozone Decay Rate ( $k(\text{O}_3)$ )

	[CFC] <sub>0</sub>	[O <sub>3</sub> ] <sub>0</sub>	$J_x$	$k_x$	$k(\text{O}_3)$	$R(\text{O}_3)$	$\alpha$
	ppm	ppm	min <sup>-1</sup>	ppb min <sup>-1</sup>	ppb min <sup>-1</sup>		
Run 1							
CFCl <sub>3</sub> (CFC-11)	5.86	4.40	$(7.3 \pm 0.4) \times 10^{-4}$	$4.3 \pm 0.2$	$75 \pm 3$	17.4	1
CF <sub>2</sub> Cl <sub>2</sub> (CFC-12)	35.69	4.61	$(1.2 \pm 0.1) \times 10^{-4}$	$4.3 \pm 0.4$	$72 \pm 3$	16.7	1.0
CF <sub>3</sub> Br (H-1301)	9.78	4.61	$(4.4 \pm 0.1) \times 10^{-4}$	$4.3 \pm 0.1$	$168 \pm 9$	39.1	2.2
C <sub>2</sub> F <sub>4</sub> Br <sub>2</sub> (H-2402)	0.85	4.26	$(5.0 \pm 0.1) \times 10^{-3}$	$4.3 \pm 0.1$	$216 \pm 19$	50.2	2.9
Run 2							
CFCl <sub>3</sub> (CFC-11)	3.92	7.67	$(2.3 \pm 0.2) \times 10^{-3}$	$9.1 \pm 0.8$	$152 \pm 4$	16.7	1
CH <sub>3</sub> CFCl <sub>2</sub> (HCFC-141b)	7.00	7.96	$(1.2 \pm 0.1) \times 10^{-3}$	$8.3 \pm 0.7$	$160 \pm 6$	19.3	1.2
CF <sub>3</sub> CHCl <sub>2</sub> (HCFC-123)	8.89	8.39	$(1.1 \pm 0.1) \times 10^{-3}$	$9.8 \pm 0.9$	$94 \pm 3$	9.6	0.6
CF <sub>3</sub> CHFCI (HCFC-124)	49.30	8.55	$(1.9 \pm 0.5) \times 10^{-4}$	$9.2 \pm 2.4$	$82 \pm 3$	9.0	0.5
CH <sub>3</sub> Br (Methyl bromide)	1.36	8.45	$(6.9 \pm 0.4) \times 10^{-3}$	$9.4 \pm 0.5$	$312 \pm 10$	33.2	2.0

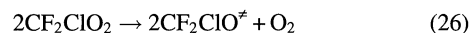
The concentrations of added CFCl<sub>3</sub> (5.9 ppm) and CF<sub>3</sub>Br (9.8 ppm) were adjusted so as to give the same formation rate for Cl and Br by the photodecomposition of CFCl<sub>3</sub> and CF<sub>3</sub>Br ( $k_x = J_x \cdot [\text{halocarbon}] = 4.3 \text{ ppb min}^{-1}$ ). Where ppb is  $10^{-3}$  ppm. As can be seen in Figs. 4 and 5, the effective ozone-depletion rate is faster in CF<sub>3</sub>Br than in CFCl<sub>3</sub>. From the slopes of the effective decay of ozone, the decay rates, ( $k(\text{O}_3)$ ) were obtained to be  $75 \pm 3$  and  $168 \pm 9 \text{ ppb min}^{-1}$  for CFCl<sub>3</sub> and CF<sub>3</sub>Br, respectively.

Similar measurements of  $k(\text{O}_3)$  were carried out for CF<sub>2</sub>Cl<sub>2</sub> and C<sub>2</sub>F<sub>4</sub>Br<sub>2</sub> under the same  $k_x$  value of  $4.3 \text{ ppb min}^{-1}$ ; all of the results are listed in Run 1 of Table 1. The ozone depletion rates, ( $k(\text{O}_3)$ ) are almost equal for CFCl<sub>3</sub> and CF<sub>2</sub>Cl<sub>2</sub>, and are faster in the BFC's. As shown in Table 1, the value of  $k(\text{O}_3)$  for C<sub>2</sub>F<sub>4</sub>Br<sub>2</sub> is larger than that for CF<sub>3</sub>Br beyond the error limits. A possible mechanism to produce an additional Br atom after the photodecomposition of C<sub>2</sub>F<sub>4</sub>Br<sub>2</sub> by reaction (8) is as follows:



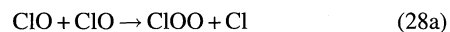
The values of  $R(\text{O}_3)$  given in Table 1 are the ratio of  $k(\text{O}_3)$  to  $k_x$ , ( $k(\text{O}_3)/k_x$ ), which indicates the number of ozone molecules decomposed per one Cl or Br atom produced by the photodissociation of the CFC's or BFC's. The number

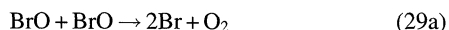
of  $R(\text{O}_3)$  was about 17 for CFCl<sub>3</sub> and CF<sub>2</sub>Cl<sub>2</sub>, and 40—50 for CF<sub>3</sub>Br and C<sub>2</sub>F<sub>4</sub>Br<sub>2</sub>. These results show that a Cl atom formed in the chamber could destroy 17 ozone molecules on the average while traveling to the wall of the chamber (on the wall of the chamber Cl atoms might be lost). In the case of the Br atom, 40—50 ozone molecules were destroyed by one Br atom during the traveling time (the photochemical chamber was a cylinder, 1450 mm in diameter, 3500 mm long, and 6065 L in volume, and gases are stirred by two stirring fans). The ozone decomposition efficiency, ( $R(\text{O}_3)$ ), were almost equal in CFCl<sub>3</sub> and CF<sub>2</sub>Cl<sub>2</sub> under the present experimental conditions. Since the formations of CFCIO and CF<sub>2</sub>O were observed as detectable reaction products by the FTIR spectrometer in systems of CFCl<sub>3</sub> and CF<sub>2</sub>Cl<sub>2</sub>, respectively, two Cl atoms might have been released from both CFCl<sub>3</sub> and CF<sub>2</sub>Cl<sub>2</sub> after photodecomposition by reactions (5) and (7). For example, the following reactions might have occurred:



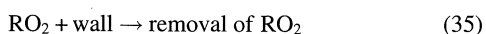
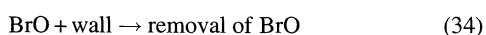
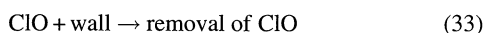
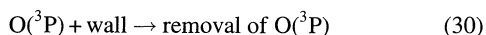
In any case, it is evident that ozone was destroyed by a catalytic cycle involving Cl or Br atoms.

The large ozone decomposition efficiency of Br compared to that of Cl might be explained by the efficiency to release Cl or Br atoms through radical-radical reactions of ClO and BrO.





The rate constant<sup>11)</sup> for reaction (29),  $2.7 \times 10^{-12} \text{ cm}^3 \text{ molecule}^{-1} \text{ s}^{-1}$ , is much faster than reaction (28),  $1.0 \times 10^{-14} \text{ cm}^3 \text{ molecule}^{-1} \text{ s}^{-1}$ , and the branching ratios in reactions (28) and (29) are  $f(28a):f(28b):f(28c)=0.34:0.17:0.49$  and  $f(29a):f(29b)=0.83:0.17$ . Therefore, the efficiency of reproducing halogen atoms through a radical-radical reaction is  $8.6 \times 10^2$  times larger in reaction (29) than in reaction (28). The longer chain length in Br atoms (40–50) than that of Cl atoms (17) can be qualitatively understood based on reactions (28) and (29). However, it is not easy to elucidate the meaning of the quantitative difference between both chain lengths. Trial box-model simulations were investigated in order to understand the mechanism of the catalytic chain reactions. In these simulations, the decay phenomena had to be adjusted by the rate of the wall reactions for  $\text{O}(^3\text{P})$ , Cl, Br, ClO, BrO, and  $\text{RO}_2$ :



**3) Box Model Simulation.** Figure 6 shows the result of a trial box-model simulation of the  $\text{O}_3 + \text{CFCl}_3 + h\nu$  system shown in Fig. 4. In this figure the concentrations of  $\text{O}_3$  in units of  $10^{12} \text{ molecule cm}^{-3}$  (not ppm) are plotted against the

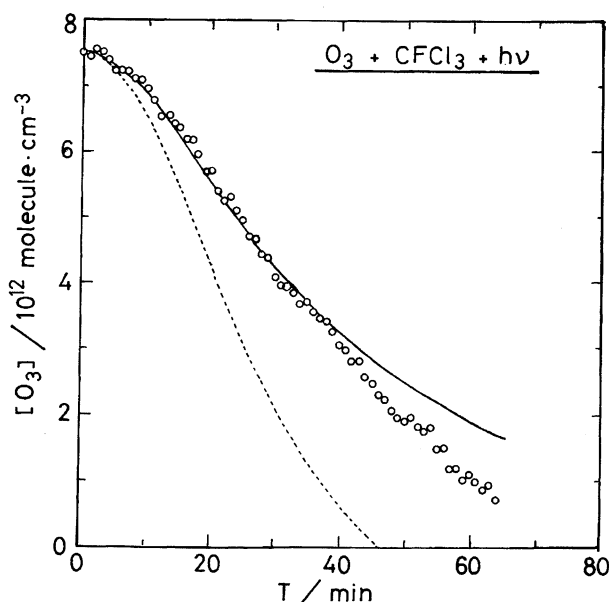


Fig. 6. Results of box model simulation of the  $\text{O}_3 + \text{CFCl}_3 + h\nu$  system. Circles show experimental results shown in Fig. 4. The dotted line shows the result of simulation without wall loss processes. The solid line shows the case including wall loss processes of  $\text{O}(^3\text{P})$ , Cl, ClO, and  $\text{RO}_2$  (see text).

reaction time (time zero is the point shown by the arrow in Fig. 4). Calculations were carried out using 42 reactions for 19 chemical species (molecules and radicals). Most of the rate data for the photodecomposition and chemical reactions among 19 chemical species are quoted from Ref. 2. The circles in Fig. 6 indicate the experimental results shown in Fig. 4. The dotted line shows the result of a simulation without wall-loss processes for all of the chemical species. The solid line indicates the case including wall-loss processes of  $\text{O}(^3\text{P})$ , Cl, ClO, and  $\text{RO}_2$  ( $2 \times 10^{-3} \text{ s}^{-1}$  was used as wall-loss rates for all four species). As can be seen in Fig. 6, if wall-loss processes are neglected, the decay of  $\text{O}_3$  obtained is much faster than the experimental results. This can be easily understood because the chain length of the catalytic cycle should be longer without any wall-loss of radicals. In Fig. 6, the solid curve (simulation) and circles (experiment) greatly differ for the latter half of the irradiation time. Probably, unknown secondary products in addition to the above mentioned 19 species might have been formed and accumulated, and additional radical reactions may have occurred by the photodecomposition of such secondary products.

The solid line in Fig. 7 shows the result of a box model simulation of the  $\text{O}_3 + \text{CF}_3\text{Br} + h\nu$  system shown in Fig. 5. The simulation involved 25 reactions of 11 chemical species. A rate of  $2 \times 10^{-3} \text{ s}^{-1}$  was used for the wall-loss processes of  $\text{O}(^3\text{P})$ , Br, BrO, and  $\text{RO}_2$ . The agreement between the experiment and simulation is much better than in the case of the Cl system (Fig. 6). In the Br system, since the decay of  $\text{O}_3$  came to completion much faster than in the Cl system, the effect of the formation of unknown secondary products might have been minor.

The concentrations of  $\text{O}(^3\text{P})$ , Cl, ClO, Br, BrO at the time that 30 and 50% of the initial  $\text{O}_3$  was decreased ( $[\text{O}_3]_t =$

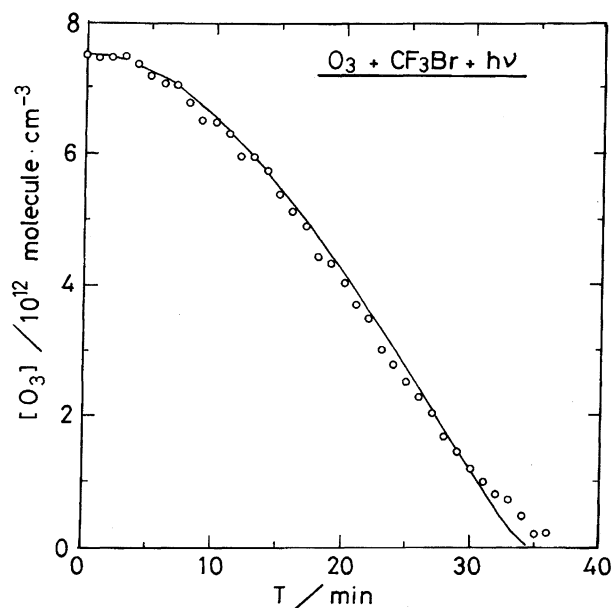


Fig. 7. Result of box model simulation of the  $\text{O}_3 + \text{CF}_3\text{Br} + h\nu$  system. Circles show experimental results shown in Fig. 5. The solid line shows the result of simulation (see text).

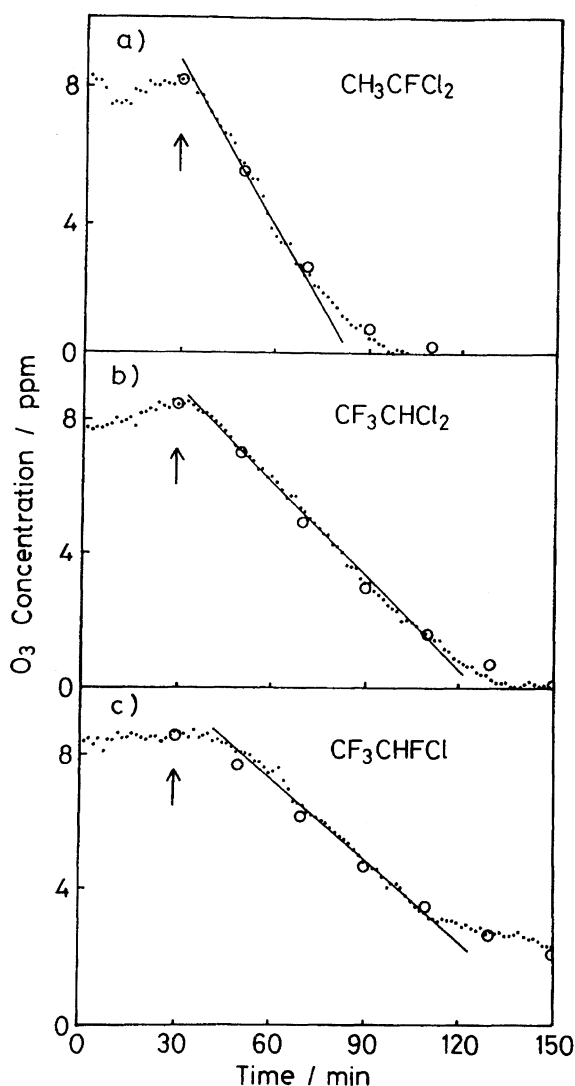


Fig. 8. Decay of ozone by the addition of (a)  $\text{CH}_3\text{CFCl}_2$ , (b)  $\text{CF}_3\text{CHCl}_2$ , and (c)  $\text{CF}_3\text{CHFCl}$ . Conditions: (a)  $[\text{CH}_3\text{CFCl}_2]_0 = 7.0$  ppm,  $k_x = 8.3$  ppb  $\text{min}^{-1}$ ,  $k(\text{O}_3) = 160 \pm 6$  ppb  $\text{min}^{-1}$ ; (b)  $[\text{CF}_3\text{CHCl}_2]_0 = 8.9$  ppm,  $k_x = 9.8$  ppb  $\text{min}^{-1}$ ,  $k(\text{O}_3) = 94 \pm 3$  ppb  $\text{min}^{-1}$ ; (c)  $[\text{CF}_3\text{CHFCl}]_0 = 49.3$  ppm,  $k_x = 9.2$  ppb  $\text{min}^{-1}$ ,  $k(\text{O}_3) = 82 \pm 3$  ppb  $\text{min}^{-1}$ .

$0.7[\text{O}_3]_0$  and  $[\text{O}_3]_t = 0.5[\text{O}_3]_0$ ) were obtained from the calculation, and are listed in Table 2. A remarkable difference between the Cl and Br systems was found at a concentration ratio of  $[\text{X}]$  to  $[\text{XO}]$ ; i.e., the ratios of  $[\text{Cl}]$  to  $[\text{ClO}]$  and  $[\text{Br}]$  to  $[\text{BrO}]$  are  $1.11 \times 10^{-3}$  and  $3.16 \times 10^{-2}$  at  $[\text{O}_3]_t = 0.7[\text{O}_3]_0$ , and  $1.49 \times 10^{-3}$  and  $5.0 \times 10^{-2}$  at  $[\text{O}_3]_t = 0.5[\text{O}_3]_0$ , respectively. In other words, the concentration of Br atoms is remarkably high in the Br system. This fact was caused by the large rate constant of Reaction (29a). From the rate constants of Reaction (17) for Cl and Br,  $3.8 \times 10^{-11}$  and  $3 \times 10^{-11}$   $\text{cm}^3 \text{ molecule}^{-1} \text{ s}^{-1}$ , respectively, and those for Reactions (28a), (28b), and (29a), and concentrations of  $[\text{O}]$  and  $[\text{XO}]$  in Table 2, the effective catalytic cycles in both systems could be estimated. In the  $\text{CFCl}_3$  system, 90% of the catalytic cycle proceeded from Reactions (16) and (17). On the other hand, in the  $\text{CF}_3\text{Br}$  system, 90% of the cycle was governed by Reactions (16) and (29a). Therefore, in the present experiment, the CFC system is relatively applicable to the atmosphere.

**4)  $\text{O}_3$  Decay by the HCFC's and  $\text{CH}_3\text{Br}$ .** Similar experiments were carried out for the HCFC's and  $\text{CH}_3\text{Br}$ . The decay of ozone in cases of  $\text{CH}_3\text{CFCl}_2$ ,  $\text{CF}_3\text{CHCl}_2$ , and

Table 3. Relative Ozone Decomposition Efficiency  $\alpha$ , Ozone Depletion Potential ODP, and Atmospheric Life-times  $\tau$

	$\alpha$	ODP	$\tau$ yrs
$\text{CFCl}_3$ (CFC-11)	1	1	55
$\text{CF}_2\text{Cl}_2$ (CFC-12)	1.0	1	116
$\text{CF}_3\text{Br}$ (H-1301)	2.2	16	65–69
$\text{C}_2\text{F}_4\text{Br}_2$ (H-2402)	2.9	7	22–30
$\text{CH}_3\text{CCl}_2\text{F}$ (HCFC-141b)	1.2	0.11	10.8
$\text{CF}_3\text{CHCl}_2$ (HCFC-123)	0.6	0.02	1.7
$\text{CF}_3\text{CHFCl}$ (HCFC-124)	0.5	0.0022	6.9
$\text{CH}_3\text{Br}$ (Methyl bromide)	2.0	0.6	1.2–1.8

Table 2. Concentrations of  $\text{O}(^3\text{P})$ , Cl, Br, ClO, and BrO radicals at time of  $[\text{O}_3]_t = 0.7[\text{O}_3]_0$  and  $[\text{O}_3]_t = 0.5[\text{O}_3]_0$

Exp. system	Reaction time s	$[\text{O}_3]_t$ $10^{12} \text{ molecule cm}^{-3}$	$[\text{O}]_t$ $10^8 \text{ molecule cm}^{-3}$	$[\text{X}]_t$ $10^8 \text{ molecule cm}^{-3}$	$[\text{XO}]_t$ $10^{10} \text{ molecule cm}^{-3}$
Time at $[\text{O}_3]_t = 0.7[\text{O}_3]_0$					
$\text{O}_3 + \text{CFCl}_3 + h\nu$	1320	5.26	2.93	$[\text{Cl}]$ 0.96	$[\text{ClO}]$ 8.68
$\text{O}_3 + \text{CF}_3\text{Br} + h\nu$	960	5.25	2.85	$[\text{Br}]$ 8.34	$[\text{BrO}]$ 2.64
Time at $[\text{O}_3]_t = 0.5[\text{O}_3]_0$					
$\text{O}_3 + \text{CFCl}_3 + h\nu$	2100	3.75	2.15	$[\text{Cl}]$ 1.43	$[\text{ClO}]$ 9.59
$\text{O}_3 + \text{CF}_3\text{Br} + h\nu$	1320	3.61	1.98	$[\text{Br}]$ 14.9	$[\text{BrO}]$ 3.00

CF<sub>3</sub>CHFCl is shown in Fig. 8. Also, results are summarized in Run 2 of Table 1. CFCI<sub>3</sub> was used as a reference in order to be able to compare Runs 1 and 2. In these experiments, the decay rates of ozone were measured under the 50 Torr air condition without hydrogen. Since the rate constant<sup>2)</sup> for reaction (16),  $1.2 \times 10^{-11}$  cm<sup>3</sup> molecule<sup>-1</sup> s<sup>-1</sup> for X = Cl, is about 10<sup>3</sup>-times faster than those for reactions<sup>2)</sup> of Cl+HCFC's, Cl atoms produced by the photodecomposition of the HCFC's react almost with ozone by reaction (16). In the case of CH<sub>3</sub>Br, Br atoms do not react with CH<sub>3</sub>Br (no exothermic reaction path).

As shown in Table 1, the ozone decay rate by CF<sub>3</sub>CHCl<sub>2</sub> is about half that by CH<sub>3</sub>CFCl<sub>2</sub>, although both compounds have two Cl atoms. The rate of ozone decay by CF<sub>3</sub>CHCl<sub>2</sub> is rather close to that by CF<sub>3</sub>CHFCl, having one Cl atom. The reaction products were measured by the FTIR spectrometer and the formation of CF<sub>3</sub>CClO was found in the case of CF<sub>3</sub>CHCl<sub>2</sub>. Therefore, only one Cl atom was released from CF<sub>3</sub>CHCl<sub>2</sub> under the present experimental conditions.

The obtained results show that the HCFC's and CH<sub>3</sub>Br can destroy ozone having sufficient potential as the CFC's and the BFC's when it entered the stratosphere, although the lifetime ( $\tau$ ) of the HCFC's in the troposphere is much shorter than that of the CFC's, as shown in Table 3, and the major part of the HCFC's and CH<sub>3</sub>Br will be destroyed in the troposphere by reaction with OH radicals.

**5) Relative Ozone Decomposition Efficiency.** The values of the relative ozone decomposition efficiency ( $\alpha$ ) normalized to CFCI<sub>3</sub> ( $\alpha=1$ ) are shown in the last column in Tables 1 and 3. In addition to the values of  $\alpha$ , the so-called ODP (ozone depletion potential) values<sup>12)</sup> obtained by the 2D-model calculations and the lifetime of each compound in the troposphere ( $\tau$ ) are listed in Table 3.

The values of  $\alpha$  should not coincide with the ODP values, because the ODP value relates not only to the chemical reactions in the stratosphere, but also to the physical global diffusion dynamics of the gases. Further, in the ODP's for the BFC's, interaction reactions between ClO and BrO were included in the calculation; also, the ODP's for the HCFC's were dominated by the reaction rate with OH in the troposphere.

### Conclusions

1. Ozone destruction by the CFC's (CFCl<sub>3</sub> and CF<sub>2</sub>Cl<sub>2</sub>), BFC's (CF<sub>3</sub>Br and C<sub>2</sub>F<sub>4</sub>Br<sub>2</sub>), HCFC's (CH<sub>3</sub>CCl<sub>2</sub>F, CF<sub>3</sub>CHCl<sub>2</sub>, and CF<sub>3</sub>CHFCl), and CH<sub>3</sub>Br was demonstrated by using a 6-m<sup>3</sup> evacuable photochemical chamber equipped with UV-enhanced Xe arc lamps.

2. Decay of ozone by a catalytic cycle involving Cl or Br atoms released from the photolysis of halocarbons by UV

light was evident although the chain length was far less than that in the real stratosphere.

3. According to the limitation of the space of the chamber, the chain length of the catalytic cycle was 8 for CFCI<sub>3</sub> and 40 for CF<sub>3</sub>Br.

4. Rates of the decomposition of ozone were faster in the BFC's than the CFC's.

5. According to the box model simulation, in the CFCl<sub>3</sub> system, 90% of the catalytic cycle proceeds from reactions of Cl+O<sub>3</sub>→ClO+O<sub>2</sub> and ClO+O→Cl+O<sub>2</sub>. On the other hand, in the CF<sub>3</sub>Br system, 90% of the catalytic cycle is governed by reactions, Br+O<sub>3</sub>→BrO+O<sub>2</sub> and BrO+BrO→2Br+O<sub>2</sub>.

6. The HCFC's and CH<sub>3</sub>Br can destroy ozone with sufficient potential as the CFC's and the BFC's when these entered into the stratosphere.

The support from the Project of the Global Environment Research Program for FY 1990—1993 of Japan Environment Agency is gratefully acknowledged.

### References

- 1) M. J. Molina and F. S. Rowland, *Nature*, **249**, 810 (1974).
- 2) W. B. DeMore, S. P. Sander, D. M. Golden, R. F. Hampson, M. J. Kurylo, C. J. Howard, A. R. Ravishankara, C. E. Kolb, and M. J. Molina, "Chemical Kinetics and Photochemical Data for Use in Stratospheric Modeling," JPL Publication 92-20; Jet Propulsion Laboratory, California Institute of Technology, Pasadena (1992).
- 3) C. H. Jackman, R. K. Seals, Jr., and M. J. Prather, "Two-Dimensional Intercomparison of Stratospheric Models," Proceedings of a Workshop Held in Virginia Beach, NASA Conference Publication 3042, National Aeronautics and Space Administration, Washington, D.C. (1988).
- 4) H. Akimoto, M. Hoshino, G. Inoue, F. Sakamaki, N. Washida, and M. Okuda, *Environ. Sci. Technol.*, **13**, 471 (1979).
- 5) S. Hatakeyama, K. Isumi, T. Fukuyama, H. Akimoto, and N. Washida, *J. Geophys. Res.*, **96**, D1, 947 (1991).
- 6) A. Miyoshi, S. Hatakeyama, and N. Washida, *J. Geophys. Res.*, **99**, D9, 18779 (1994).
- 7) P. Warneck, "Chemistry of the Natural Atmosphere," Academic Press, Inc., San Diego (1987), pp. 61—70.
- 8) T. J. Wallington and M. D. Hurley, *Chem. Phys. Lett.*, **189**, 437 (1992).
- 9) E. C. Tuazon, R. Atkinson, and S. B. Corchnoy, *Int. J. Chem. Kinet.*, **24**, 639 (1992).
- 10) R. F. Warren and A. R. Ravishankara, *Int. J. Chem. Kinet.*, **25**, 833 (1993).
- 11) R. Atkinson, D. L. Baulch, R. A. Cox, R. F. Hampson, Jr., J. A. Kerr, and J. Troe, *J. Phys. Chem. Ref. Data*, **18**, 881 (1989).
- 12) "Scientific Assessment of Stratospheric Ozone: 1991," World Meteorological Organization, Global Ozone Research and Monitoring Project, Report No. 25.